# New Epitopes and Comparative Analysis of Children and Murine Immune Responses to Pertussis Toxin Subunits (S1–S5) Induced by Whole-Cell Pertussis Vaccination

Salvatore G. De-Simone *, Guilherme C. Lechuga, Paloma Napoleão-Pêgo, Mariana S. Freitas, Sergian V. Cardoso, Carlos M. Morel, David W. Provance Jr, Flavio R. Silva

Posted Date: 26 February 2026

doi: 10.20944/preprints202602.1259.v1

Keywords: *Bordetella pertussis*; pertussis toxin S1-S5 subunits; infants and mice epitope mapping; peptide array; SPOT-synthesis

 doi:10.20944/preprints202602.1259.v1



*Article*

# New Epitopes and Comparative Analysis of Children and Murine Immune Responses to Pertussis Toxin Subunits (S1–S5) Induced by Whole-Cell Pertussis Vaccination

**Salvatore G. De-Simone [1,2,3,*], Guilherme C. Lechuga [1], Paloma Napoleão-Pêgo [1], Mariana S. Freitas [1,2], Sergian V. Cardoso [4], Carlos M. Morel [1], David W. Provance Jr [1] and Flavio R. Silva [1]**

[1] Center for Technological Development in Health (CDTS)/ National Institute of Science and Technology for Innovation in Neglected Population Diseases (INCT-IDPN), FIOCRUZ, Rio de Janeiro, RJ, 21040-900

[2] Program of Post-Graduation on Science and Biotechnology, Department of Molecular and Cellular Biology, Biology Institute, Federal Fluminense University, Niteroi 22040-036, Brazil

[3] Program of Post-Graduation on Parasitic Biology, Oswaldo Cruz Institute, Oswaldo Cruz Foundation, Rio de Janeiro 21040-900, Brazil

[4] Program in Translational Biomedicine (BIOTRANS), Graduate Department of Health, University of Grande Rio (UNIGRANRIO), Caxias 25071-202, Brazil

* Correspondence: salvatore.simone@fiocruz.br

**Abstract**

Pertussis toxin (Ptx) is a key virulence factor and protective antigen of *Bordetella pertussis*. Understanding its antigenic landscape is critical for improving vaccine formulations. This study compared the antigenic mapping of continuous epitopes recognized by children and murine antibodies against Ptx subunits S1–S5. Two libraries of nine overlapping 14-mer peptides encompassing the full-length Ptx sequence were synthesized to identify linear antibody-binding regions. Antibodies from children and mice immunized with whole-cell pertussis vaccine recognized several common, though not identical, epitopes. Some regions were species-specific, while shared epitopes exhibited minor positional shifts, indicating subtle differences in recognition. Eighteen major epitopes were recognized by vaccinated mice and twenty-six by the serum of vaccinated children. Eleven present shared sequences [S1 (Ep3-5,7,9,10); S3 (20,21,25,26); S5 (Ep 30)], and eight were recognized uniquely by the serum of children's [S1 (Ep1,6,8); S3 (Ep22-Ep24) and S4 (Ep27,29-30)]. Four unique and distinct epitopes were identified in the S2 subunit for each species [mice Ep11,14,16,17 and children Ep12,13,15,18, and only one in the S4 subunit [mice Ep 28]. Structural analysis revealed a non-uniform antibody recognition of pertussis toxin, with dominant targeting of the S3 subunit and conserved epitope hotspots, alongside a distinct subset of antibodies engaging the catalytic S1 subunit, providing structural evidence for multiple neutralization mechanisms. These findings provide a mechanistic basis for differences in toxin neutralization and highlight limitations in extrapolating murine epitope data to human immunity. The conserved antigenicity of the subdomains provides valuable insights into Ptx immunogenicity and represents promising candidates for inclusion in next-generation synthetic pertussis vaccine design.

**Keywords:** *Bordetella pertussis*; pertussis toxin S1-S5 subunits; infants and mice epitope mapping; peptide array; SPOT-synthesis

 doi:10.20944/preprints202602.1259.v1



## 1. Introduction

Pertussis is a pulmonary disease caused by the gram-negative bacterium Bordetella pertussis, with a high fatality rate among newborns and young children. Pertussis toxin (Ptx) is essential for pertussis pathogenesis, a major immunogen of *B. pertussis*, and a key antigen in both whole-cell (wP) and acellular (aP) pertussis vaccines [1,2]. Comparative studies of the immune response to Ptx in mice and humans provide valuable insights into host-specific mechanisms of protection, the nature of antibody repertoires, and the translational relevance of animal models used in pertussis research [3]. Although both species develop antibody-mediated immunity following vaccination or infection, significant quantitative and qualitative differences may occur in the specificity, magnitude, and persistence of these responses [4–6].

In mice, immunization with the whole-cell DTP vaccine induces a robust, polyclonal antibody response against multiple Ptx subunits (S1–S5) and other bacterial antigens, such as filamentous hemagglutinin and pertactin [7]. The murine humoral response is characterized predominantly by IgG2a and IgG2b subclasses, reflecting a Th1/Th17-skewed immune profile typical of responses to complex bacterial antigens [5,8–10]. This response promotes opsonization and complement activation, contributing to efficient bacterial clearance. However, mice also generate mucosal IgA antibodies [11–13], particularly after intranasal or whole-cell vaccination, that can neutralize Ptx at the site of infection [11–14]. However, the repertoire of recognized epitopes tends to be narrower, with preferential targeting of conserved and surface-exposed regions of the S2, S3, and S4 subunits, rather than the enzymatic domains of S1.

In children, both natural infection and vaccination elicit a strong antibody response to Ptx, but the pattern of immunodominance differs [15,16]. Human sera typically show high titers of IgG1 and IgG4, consistent with a Th2-biased response, especially following acellular vaccination. Individuals vaccinated with whole-cell formulations, however, produce a more balanced IgG1/IgG3 response, associated with greater neutralizing capacity [6]. Importantly, human antibodies can recognize conformational epitopes spanning multiple subunits of Ptx, particularly within the S1 enzymatic domain [17] and the receptor-binding interface of S2 and S3 [18]. This suggests that the human immune system may rely more on tertiary and quaternary structural determinants than on linear epitopes, as is often observed in murine sera.

However, it has been documented that murine antisera [19] or monoclonal antibodies [20–23] tend to recognize linear and conserved peptide sequences, particularly within the B oligomer subunits (S2, S3, S4), suggesting a focus on structural motifs accessible on the toxin surface. In contrast, children's sera identify both linear and discontinuous epitopes, often overlapping with receptor-binding or enzymatically active domains, which may contribute to the generation of neutralizing antibodies that inhibit Ptx activity [20,22]. These differences reflect not only species-specific B cell repertoires but also distinct antigen processing and presentation pathways [23].

Functionally, both murine and children's antibodies can neutralize Ptx, but the efficiency and persistence of this response differ [21]. Children typically exhibit longer-lasting serum antibody titers and memory responses, particularly following booster vaccination or natural infection [24,25]. In mice, antibody levels peak rapidly after immunization but decline more quickly, consistent with a shorter-lived plasma cell response [26,27]. Nevertheless, the murine model remains valuable for dissecting the mechanisms of protection and for mapping linear B-cell epitopes relevant to vaccine-induced immunity.

Thus, the qualitative identification of specific antigenic regions recognized by antibodies in both species is essential for the rational design of safer, more effective next-generation vaccines. Epitope mapping studies further highlight these interspecies distinctions. Understanding these interspecies differences is essential for translating findings from animal models to children's immunity and for guiding the rational design of next-generation pertussis vaccines that elicit durable, cross-protective antibody responses.

 doi:10.20944/preprints202602.1259.v1



## 2. Materials and Methods

### *2.1. Immunization of Mice*

To obtain mouse sera, 38 NIH Swiss mice weighing 12-16 g were immunized as previously described [28] with a whole-cell vaccine tetra-valent (DTP-HepB/Hib) from the National Immunization Program. The vaccine, administered in 0.5 ml doses containing 2 IU (as defined by the Brazilian National Immunization Program), was given at 21-day intervals. Sera were collected 1 week after the final inoculation and stored at -20°C.

The procedures involving the animals and their care were conducted in accordance with the Guidelines for the Use of Animals in Biochemical Research and were approved by the institutional ethical committee (CEUA 052/2021).

### *2.2. Human Sera*

Ninety-two children aged 1–12 years (median age 7.5 years; group A, 1–4 y, group B, 5–9 y, and group C, 10–13 y) vaccinated with the whole DTP (diphtheria/tetanus/pertussis) with no evidence of acute infection or known history of whooping cough and diphtheria were enrolled in this study. This study also included one hundred serum samples from healthy blood bank donors (HEMORIO). This study was approved by the UNIGRANRIO (CAAE: 24856610.0.0000.5283) study center ethics committee and conducted in accordance with good clinical practice and all applicable regulatory requirements, including the Declaration of Helsinki.

### *2.3. Synthesis of the Cellulose-Membrane-Bound Peptide Array*

Two libraries of 192 amino acids overlapping fourteen peptides, frameshifted by 5 residues, covering the primary sequence of S1 (P04977.1), S2 (P04978.2), S3 (P04979.1), S4 (P0A3R5.1), S5 (P04981.5), Ptx were synthesized directly onto amino-PEG500-UC540 cellulose membranes. This was achieved using the SPOT synthesis technique, as previously described [29], with an Auto-Spot Robot ASP-222 (Intavis Bioanalytical Instruments AG, Köln, Germany) and the F-moc strategy. For the immunodetection assays, the membranes were washed with TBS (50 mM Tris-buffer saline, pH 7.0) and blocked overnight with TBS-CT (Tris-buffer saline, 3% casein, 0.1% Tween 20, pH 7.0) at room temperature under agitation or overnight at 4 °C. After extensive washing with TBS-T (Tris-buffer saline, 0.1% Tween 20, pH 7.0), to remove any unbound or non-specifically bound peptides the membranes presenting the peptide libraries were incubated for 2 h with a pool of mice or children vaccinated sera (1:100) in TBS-CT and then washed again with TBS-T. The membranes were used immediately. Negative controls (without peptide; IHLVNNESSEVIVH K (*Clostridium tetani*) precursor peptide) and positive controls (GYPKDGNAFNNLD RI-*Clostridium tetani*–A10 and KEVPALTAVE TGATN–Poliovirus–A11) were included.

### *2.4. Screening and Measurement of Spot Signal Intensities*

SPOT membranes were equilibrated with PBS-T (phosphate-buffered saline, 0.1% Tween 20, pH 7.4) and blocked with 3% BSA in PBS-T for 1 h at room temperature or overnight. After extensive washing with PBS-T, membranes were incubated for 1 h with goat anti-mouse IgG (KPL, Gaithersburg, MD, USA) or goat anti-human IgG (Sigma-Aldrich, St Louis, Mo, USA) conjugated to alkaline phosphatase (1:5000) for 1 h at 37 °C, followed by washing with TBS-T and CBS (50 mM citrate-buffer saline, pH 7.0). To complete the reaction, chemiluminescent CDP-Star® Substrate (0.25 mM) with Nitro-Block-II™ Enhancer (Applied Biosystems, Waltham, Massachusetts, USA) was added.

Chemiluminescent signals were scanned and measured using an Odyssey FC (LI-COR Bioscience, Lincoln, NE, USA), as previously described [30]. In brief, a 5 MP digital image file was generated, and signal intensities were quantified using TotalLab TL100 (v. 2009; Nonlinear Dynamics,

 doi:10.20944/preprints202602.1259.v1



Newcastle upon Tyne, UK) software. The signal intensity (SI) used as a background was determined by a set of negative controls spotted on each membrane.

### *2.5. Bioinformatics Analysis and in Silico Models*

The complete protein sequences of interest [subunits S1 (P04977.1), S2 (P04978.2), S3 (P04979.1), S4 (P0A3R5.1), S5 (P04981.5)] of the Ptx were initially retrieved from the National Center for Biotechnology Information, USA (http://www.ncbi.nlm.nih.gov, accessed September 10, 2025).

To identify epitope locations within the 3D structures of these proteins, we generated models using UCSF ChimeraX, Version 1.11 (https://www.rbvi.ucsf.edu/chimerax/; accessed on 20 September 2025). The structures of the five proteins were generated using the AlphaFold server [31] and the Protein Data Bank (PDB). Searches for pertussis toxin subunits were conducted in the Protein Information Resource (PIR) database (https://research.bioinformatics.udel.edu/peptidematch/index.jsp, accessed on 10 November 2025) using previously identified sequences in other organisms.

Similarity analysis with proteins from other organisms was conducted using BLASTP version 4.0. Multiple sequence alignments were performed using the programs ClustalW (http://www.ebi.ac.uk/clustalw) and BioEdit (http://www.mbio.ncsu.edu/ BioEdit/ bioedit.html).

### *2.6. Structural Modeling of Pertussis Toxin and Epitope Mapping*

The three-dimensional structure of the Ptx-S1 was obtained from experimentally resolved structural data deposited in the PDB. Structural analyses were conducted using PyMOL (Schrödinger LLC, New York, NY, USA) and UCSF ChimeraX to delineate the architecture of the enzymatically active center responsible for $NAD^+$-dependent ADP-ribosyltransferase activity.

### *2.7. Antigen–Antibody Interface*

Structural complexes of *Bordetella pertussis* toxin bound to neutralizing antibodies were identified by searching the Protein Data Bank (PDB). A total of five unique antibody–antigen complex structures were retrieved and analyzed: 9MR7, 9E3L, 9E3H, 9E3J, and 9E3K. Duplicate entries were excluded from subsequent analyses.

The selected structures were used to investigate the binding mode of antibody fragments (Fabs) to pertussis toxin subunits and to characterize interactions involving previously identified or putative epitopes. Structural visualization, inspection, and comparative analyses were performed using UCSF ChimeraX (version 1.11) and PyMOL (Schrödinger, version 4.6.0). These tools were employed to examine antibody orientation, paratope–epitope complementarity, and the contribution of individual complementarity-determining regions (CDRs) to antigen recognition.

A refined and systematic analysis of non-covalent interactions at the antigen–antibody interface was conducted using the Protein–Ligand Interaction Profiler (PLIP) web server. PLIP was used to identify and classify intermolecular interactions, including hydrogen bonds, electrostatic (salt-bridge) interactions, hydrophobic contacts, π–π stacking, and cation–π interactions, based on side-chain geometry and distance criteria. Interaction profiles were generated for each complex and compared to identify conserved binding features and structural determinants associated with antibody neutralization.

## 3. Results

### *3.1. Epitope Mapping*

Epitopes in the Ptx subunit protein (total of 960 residues) were identified based on recognition of peptides in synthesized libraries by children's and murine antibodies immunized with a wPv. **Figures 1-5**, Panels B and C present the position of each peptide derived from each subunit (PtxS1, PtxS2, PtxS3, PtxS4, and Ptx5) and the measured intensity (panels A) from the chemiluminescent

 doi:10.20944/preprints202602.1259.v1



detection of mice and children's IgG antibodies in sera pooled from vaccinated with the wPv. The intensities were normalized to 100% using the positive control.

A list of the Ptx subunit peptides sequences synthesized and their positions on the membranes is presented in Figure S1. The pattern of reactivity for the antibodies generated in children vaccined with the wPv demonstrated that more peptides were recognized than in mice immunized with the wPv vaccine (Table 1).

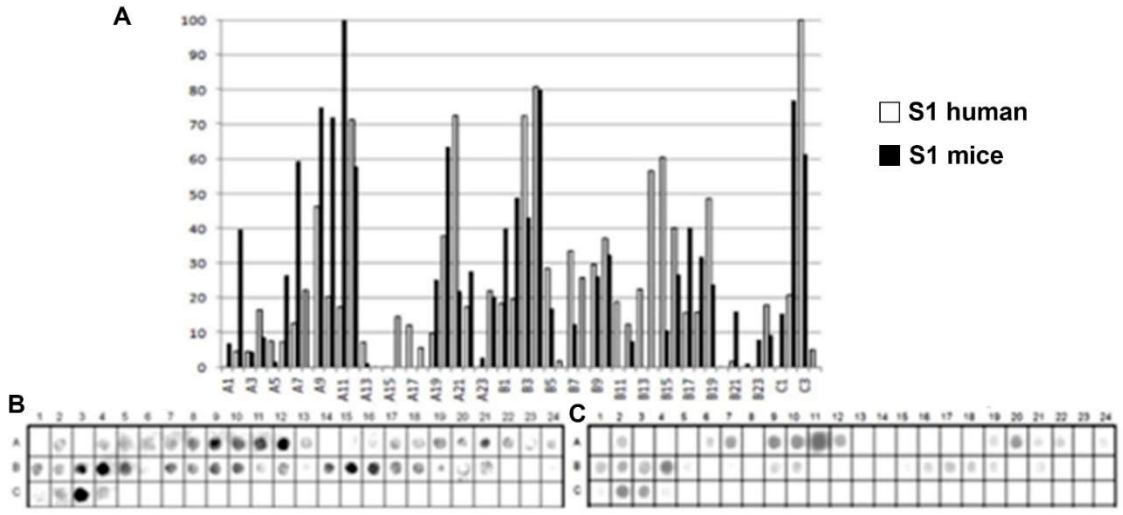


**Figure 1.** Epitope mapping of the PtxS1. (A) Quantitative analysis of chemiluminescent signal intensity from peptide array membranes incubated with pooled sera from miVs and chVs. (B, C) Digital image of the peptide array membrane synthesized in parallel and incubated with chVs (B) and miVs. Each spot corresponds to a 14–amino acid peptide overlapping by 9 residues, collectively spanning the entire PtxS1 sequence.

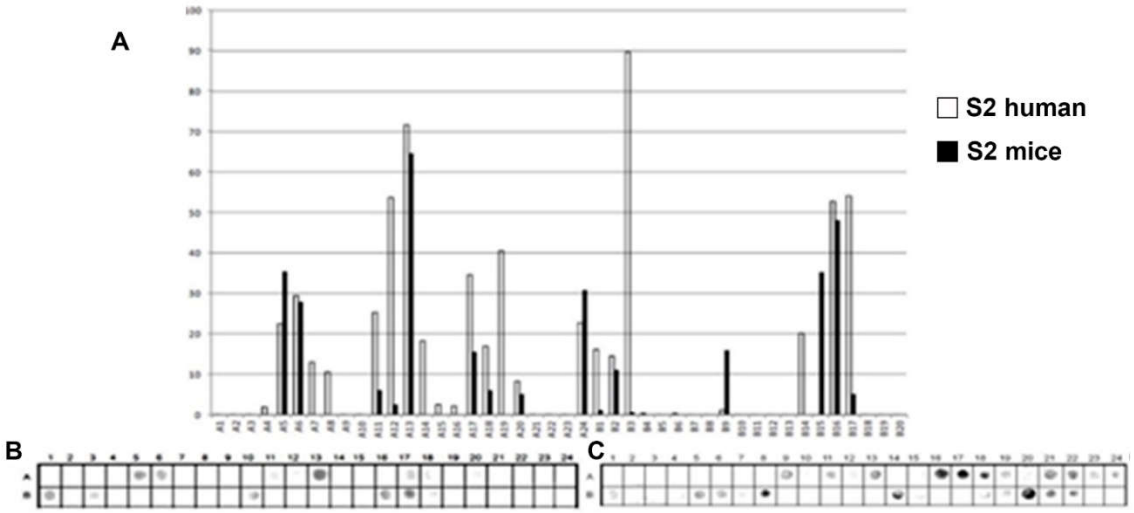


**Figure 2.** Epitope mapping of the PtxS2. (A) Quantitative analysis of chemiluminescent signal intensity from peptide array membranes incubated with pooled sera from miVs and chVs. (B, C) Digital image of the peptide array membrane synthesized in parallel and incubated with chVs (B) and miVs. Each spot corresponds to a 14–amino acid peptide overlapping by 9 residues, collectively spanning the entire PtxS1 sequence.

 doi:10.20944/preprints202602.1259.v1



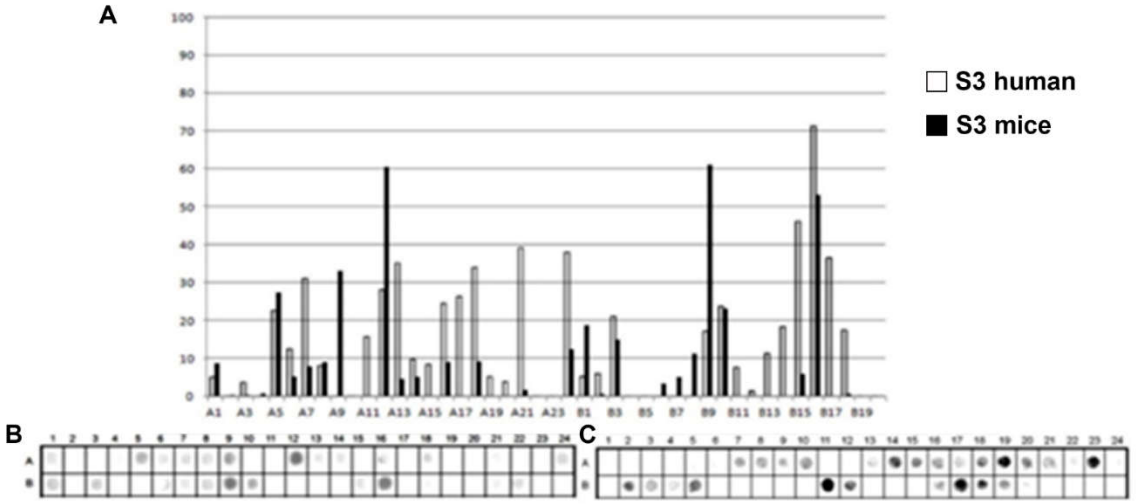


**Figure 3.** Epitope mapping of the PtxS3. (A) Quantitative analysis of chemiluminescent signal intensity from peptide array membranes incubated with pooled sera from miVs and chVs. (B, C) Digital image of the peptide array membrane synthesized in parallel and incubated with chVs (B) and miVs. Each spot corresponds to a 14–amino acid peptide overlapping by 9 residues, collectively spanning the entire PtxS1 sequence.

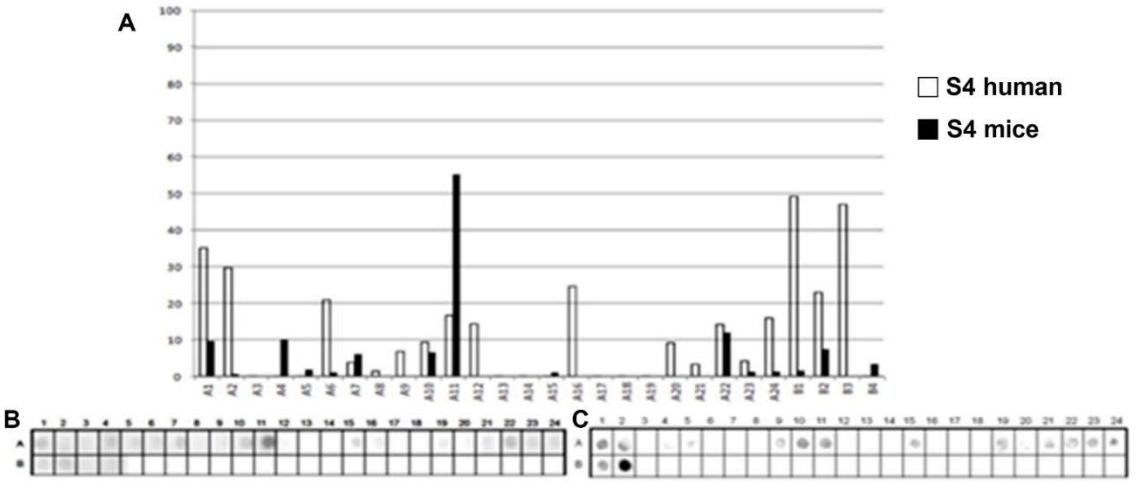


**Figure 4.** Epitope mapping of the PtxS4. (A) Quantitative analysis of chemiluminescent signal intensity from peptide array membranes incubated with pooled sera from miVs and chVs. (B, C) Digital image of the peptide array membrane synthesized in parallel and incubated with chVs (B) and miVs (C). Each spot corresponds to a 14–amino acid peptide overlapping by 9 residues, collectively spanning the entire PtxS1 sequence.

 doi:10.20944/preprints202602.1259.v1



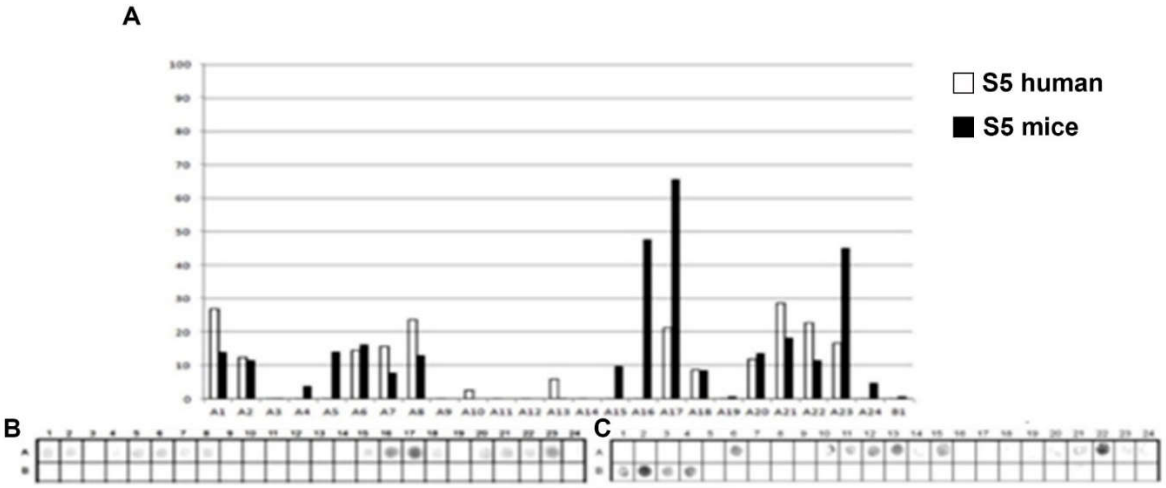


**Figure 5.** Epitope mapping of the PtxS5. (A) Quantitative analysis of chemiluminescent signal intensity from peptide array membranes incubated with pooled sera from miVs and chVs. (B, C) Digital image of the peptide array membrane synthesized in parallel and incubated with chVs (B) and miVs. Each spot corresponds to a 14–amino acid peptide overlapping by 9 residues, collectively spanning the entire PtxS1 sequence.

An analysis of peptide sequences synthesized in reactive regions identified 19 epitopes recognized by miVS and 23 by children's vaccinated sera (chVs) (**Table 1).** Six epitopes were uniquely specified by the miVs (Ep11,14,16,17,19) and thirteen by the chVs (Ep1,6,8,12,13,15,18,22-24,28,31,32). The remaining epitopes were common between the two species (Table 1). Overall, the epitopes were designated as Ep1-Ep32 for this study.

*3.2. Localization of the B-Epitopes Within the Ptx Protein*

A total of 32 linear B-epitopes were identified by SPOT-synthesis analysis in the sera of children and/or vaccined mice. The Ptx protein gene contains five well-defined chains: S1 (269 residues), S2 (226 residues), S3 (227 residues), S4 (227 residues), and S5 (133 residues). Nine epitopes (Ep1, Ep3-10) were identified by the chVs, and eight (Ep2-5 and Ep7, Ep9, and Ep10) by miVs, in the PtxS1 chain. Four epitopes (Ep12, Ep13, Ep15, Ep18) were detected by chVs and four (Ep11, Ep14, Ep16 and Ep17) in the PtxS2. Six (Ep20-Ep26) were detected by chVs, and four (Ep19-Ep21, Ep25, and Ep26) by miVs in PtxS3. In S4, only one epitope was reactive to miVs (Ep28), and neither to chVs; three epitopes (Ep27, Ep29-Ep30) were identified exclusively for chVs (Table 1). Two epitopes were found in S5 for miVs (Ep 31 and 32), and Ep32 was shared by chVs.

The shared epitopes in the PtxS1 were six (Ep3, Ep4, Ep5, Ep7, Ep9, and Ep10), in the PtxS2 (none), in the PtxS3 (four; Ep20, Ep21, Ep25, and Ep26), PtxS4 (none), and in the PtxS5 (one; Ep32) (Table 1).

**Table 1.** Relationship of Ptx IgG epitopes identified by sera from cellular pertussis vaccinated mice (miVs) and children (chVs).

| Epitope number | Ptx-S1 mice | S1-children | Cross reactivity | References |
|---|---|---|---|---|
| Ep1 | | $^{11}$ARTGWLTWLA$^{20}$ | | aa 3-16/mAb [32] and Rab* [33] |
| Ep2 | $^{31}$PAWADDPPA$^{39}$ | | | |
| Ep3 | $^{46}$SRPPEDVFQNGFTAW GNND$^{64}$ | $^{61}$GNNDNVLDHL$^{70}$ | | |

 doi:10.20944/preprints202602.1259.v1



| | | | | |
|---|---|---|---|---|
| Ep4 | 96VYLEHRMQEAVEAE109 | 105AVEAERAGRGTGH117 | BPp | |
| Ep5 | 126RADNNFYGAASSYFEYVDT144 | 136SSYFEYVDTYGDNA149 | BPp | aa 121-138/Rab* [32] |
| Ep6 | | 156ALATYQSEY164 | BPp | |
| Ep7 | 166AHRRIPPEN174 | 170IPPENIRRVT179 | BPp | |
| Ep8 | | 191TTTEYSNAR199 | BPp | |
| Ep9 | 201VSQQTRANPNPYTSRRSVA219 | 211PYTSRRSVASIVGT224 | BPp | aa 211-222 /Rab* [33]<br>aa 201-235/mice [32] |
| Ep10 | 251ERAGEAMVL259 | 251ERAGEAMVLVYYES264 | BPp | |
| | S2 mice | S2-children | | |
| Ep11 | 26RASTPGIVI34 | | BPp | aa 1-23/Rab* [34] |
| Ep12 | | 66GDLQEYLRH74 | BPp | |
| Ep13 | | 91GGEYGGVIKDGTPG104 | BPp | |
| Ep14 | 121TGQPATDHY129 | | BPp | |
| Ep15 | | 131SNVTATRLLSSTNS144 | BPp | aa134-149/<br>Rab*[35] |
| Ep16 | 161CTSPYDGKYWSMYS174 | | BPp | |
| Ep17 | 195SKEEQYYD202 | | | aa 186-199/<br>Rab* [35] |
| Ep18 | | 205DATFETYALT214 | | |
| | S3- mice | S3-children | | |
| Ep19 | 21LGMRTAQAVAPGIVIPPKAL34 | | BPp | aa 18-41/Rab* [34] |
| Ep20 | 41FTQQGGAYGRC51 | 31PGIVIPPKALFTQQ44 | BPp | aa 37-64/Rab* [34] |
| Ep21 | 56RALTVAELRGNAEL69 | 66NAELQTYLR74 | BPp | |
| Ep22 | | 86YDGTYGQAYGGII99 | BPp | |
| Ep23 | | 106AGFIYRETF114 | BPp | |
| Ep24 | | 116ITTIYKTGQPAADH1 | BPp | |
| Ep25 | 161ACASPYEGRYRDMY174 | 169YRDMYDALRR179 | | aa 149-176/Rab* [34] |
| Ep26 | 196SKEEQYYDYED206 | 200QYYDYEDATF209 | | |
| | S4-mice | S4-children | | |
| Ep27 | | 06PTRTTAPGQ14 | | |
| Ep28 | 56TSVAMKPYEVTPTR69 | | | |
| Ep29 | | 125GPKQLTFEGK134 | | |
| Ep30 | | 136ALELIRMV143 | | |

 doi:10.20944/preprints202602.1259.v1



| | S5- mice | S5-children | | |
|---|---|---|---|---|
| **Ep31** | **[76]LSDAGHEHDTWFDTM LGFA[9]** | | | |
| **Ep32** | **[111]SPYPGTPGDLLEL[123]** | **[106]LTVEDSPYP[114]** | | |

•Rabbit antisera raised against synthetic peptides; BPp, *Bordetella parapertussis*; mAb, monoclonal antibodies. The common epitope residues recognized by both species are shown in yellow.

### *3.3. Spatial Location of the Ptx Reactive Epitopes*

The tridimensional structures of mature Ptx have been determined to a resolution of 2.5 ˚A by X-ray diffraction [36,37]. In our study, a predicted structural model of the S1-S5 subunits was obtained (Figure 6) using AlphaFold and displays the spatial localization of the most reactive epitopes identified by the SPOT-synthesis array experiments. Most of the linear epitopes were in coil/loop structures in the S1-S5 protein structure. The hydropathy plots of the Ptx subunits also suggested that all epitopes were on the surface of the proteins

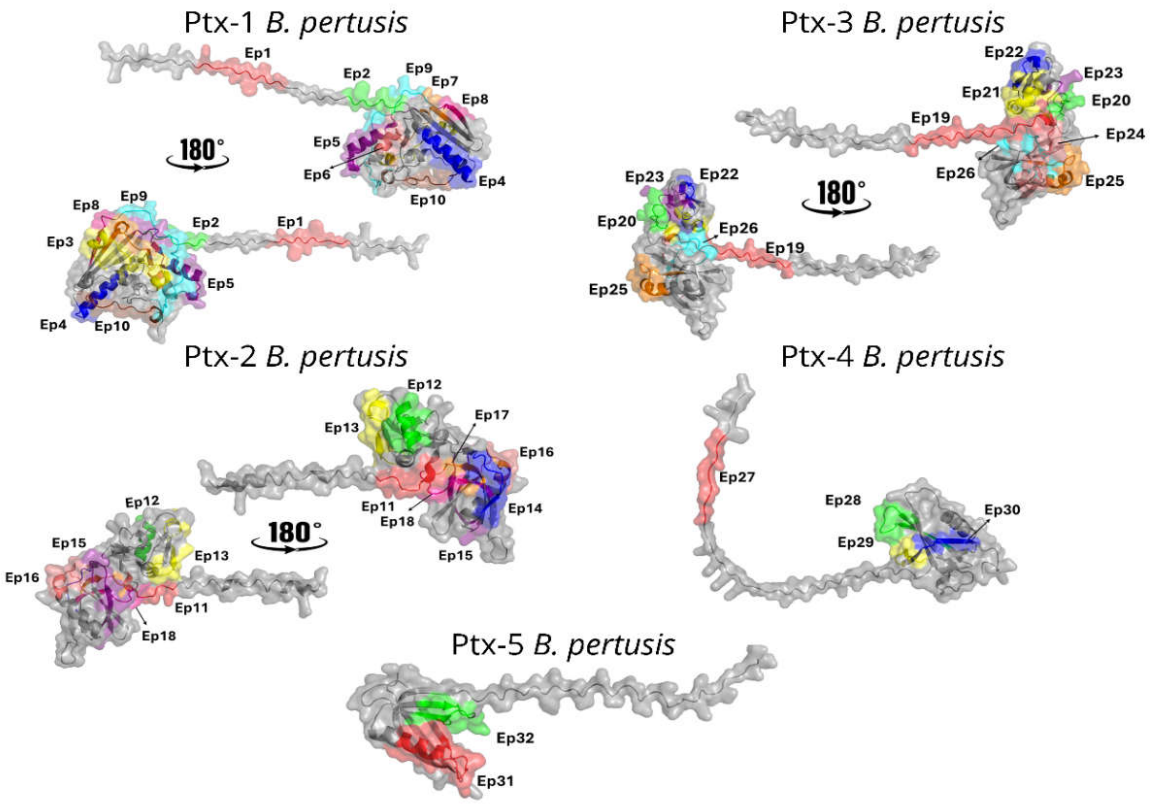


**Figure 6.** Spatial distribution of IgG reactive epitopes. The figure depicts the spatial positioning of children- and mouse-IgG-reactive epitopes (Table 1) within the S1-S5 domain of the Ptx.

### *3.4. Distribution of Antibody Binding Across Ptx and Epitope Hotspots*

Analysis of the available pertussis toxin–antibody complex structures revealed a non-uniform distribution of antibody binding across toxin subunits. Antibody interactions were predominantly observed with subunit S3, which accounted for the most binding events (N = 16), indicating that this subunit represents a major immunogenic and structurally accessible region of the toxin. In contrast, subunits S2 and S4 showed a moderate number of antibody interactions (n= 7 each), suggesting secondary but relevant roles in antibody recognition. Only a single antibody interaction was detected for subunit S1 (n=1), indicating limited structural targeting of this subunit by neutralizing antibodies

 doi:10.20944/preprints202602.1259.v1



within the currently available structural dataset. Interesting to note that S1 represents the catalytic domain, the Ep5 (residues 136–149) was located within the core of the catalytic cleft, whereas Ep3 (residues 63–70) and Ep4 (residues 105–113) occupied adjacent loops and secondary structural elements that frame the active site. Together, these regions define an extended functional epitope spanning the toxin's enzymatic center.

At the epitope level, interaction mapping identified distinct epitope hotspots that were repeatedly targeted by multiple antibodies. Epitopes Ep23 and Ep24 emerged as the most frequently recognized regions, each interacting with five independent antibodies, highlighting their potential role as dominant antigenic sites. Epitope Ep15 showed intermediate recognition (n=3), while a group of epitopes (Ep12, Ep13, Ep20, Ep27, Ep29, and Ep30) displayed moderate antibody engagement (N=2 each). The remaining epitopes (Ep18, Ep21, Ep22, Ep25, Ep28, and Ep4) were each recognized by a single antibody, suggesting more restricted or context-dependent accessibility (Figure 7).

### *3.5. Structural Basis of Toxin Neutralization*

Antibody-mediated neutralization of pertussis toxin can occur through multiple mechanisms, including steric hindrance of receptor binding, destabilization of toxin assembly, or direct interference with the catalytic activity of the enzymatic subunit. Although most antibody interactions identified in this study were concentrated on the S2, S3, and S4 subunits, a limited but noteworthy interaction with the S1 subunit, which harbors the catalytic domain, was observed. Given the central role of S1 in ADP-ribosyltransferase activity, antibodies targeting this subunit may directly inhibit toxin function.

To explore this possibility, we performed a detailed structural analysis of PDB entry 9MR7, which corresponds to the monoclonal antibody hu1B7 bound to epitope Ep4 on the S1 subunit. This antibody has been reported to recognize both human and murine pertussis toxin, making it particularly relevant for functional interpretation. Structural inspection revealed that hu1B7 engages the catalytic subunit through a network of specific non-covalent interactions involving both the light and heavy chains.

The light chain contributes to antigen recognition through a combination of hydrophobic contacts, hydrogen bonds, and π–cation interactions. A hydrophobic interaction involving residue HIS117A was detected at a distance of 3.65 Å, suggesting stabilization of the antibody–toxin interface. In addition, hydrogen bonds formed by GLY114A (2.56 Å) and THR115A (2.99 Å) further anchor the antibody to the epitope. A π–cation interaction involving ARG113A at 4.74 Å likely reinforces binding specificity and orientation.

The heavy chain establishes additional stabilizing contacts through hydrogen bonds involving GLY112A (3.18 Å) and ARG113A (1.92 Å). Notably, the short interaction distance observed for ARG113A indicates strong, potentially functionally relevant contact that may constrain the local conformational flexibility of the S1 subunit.

Importantly, the localization of Ep4 within the S1 subunit places these interactions near the catalytic region of the toxin, suggesting a neutralization mechanism based on direct steric obstruction or conformational restriction of the enzymatic domain (Figure 7). Such binding may impair substrate access or disrupt the proper positioning of residues required for ADP-ribosyltransferase activity. Together, these findings support a model in which a subset of neutralizing antibodies directly targets the catalytic subunit, providing an additional, mechanistically distinct layer of toxin neutralization.

 doi:10.20944/preprints202602.1259.v1



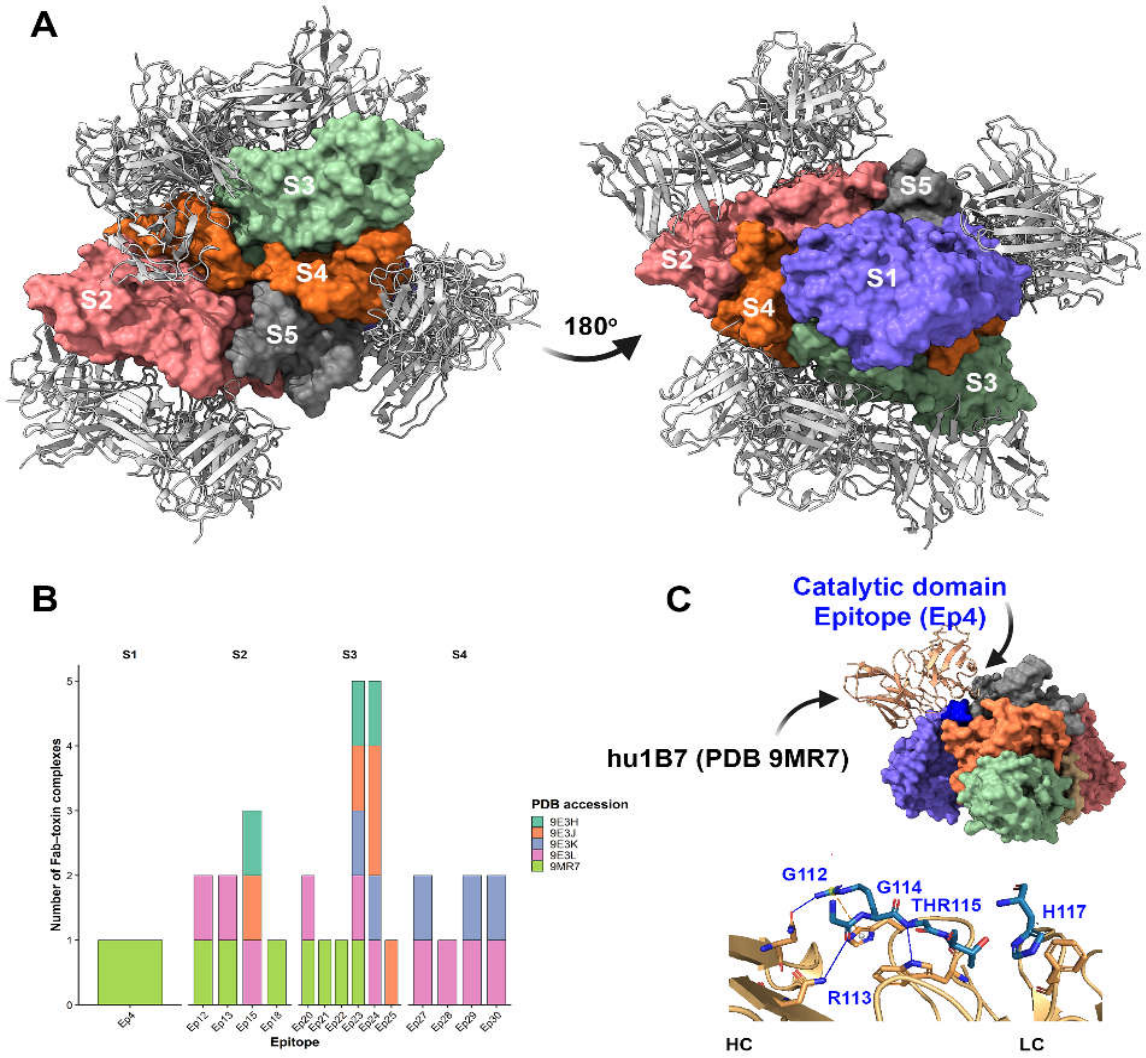


**Figure 7.** Structural and quantitative analysis of pertussis toxin–antibody interactions. (A) Structural overview of Ptx in complex with neutralizing antibody Fab fragments derived from five deposited crystal or cryo-EM structures (PDB IDs: 9MR7, 9E3L, 9E3H, 9E3J, and 9E3K). The toxin subunits (S1–S5) are shown as surface or cartoon representations, with bound Fab fragments displayed to highlight differences in antibody orientation and subunit specificity across complexes. (B) Quantitative distribution of antibody binding across pertussis toxin subunits. The number of antibodies interacting with each subunit (S1–S5) was determined from structural analyses, revealing a predominant targeting of the S3 subunit, followed by S2 and S4, with limited binding to the catalytic S1 subunit. (C) Detailed interaction map of the monoclonal antibody hu1B7 bound to the S1 subunit at epitope Ep4 (PDB ID: 9MR7). The antibody light chain (LC) and heavy chain (HC) are shown engaging the catalytic subunit through a network of non-covalent interactions. Hydrogen bonds are depicted as blue dashed lines, while π–cation interactions are shown as yellow dashed lines, illustrating the molecular basis of antibody recognition and the potential interference with the toxin's enzymatic activity.

### *3.6. Cross-Immunity Conferred with Other Strains of B pertussis*

To investigate the cross-immunity conferred by the PtxS1-S5 subunits of *B. pertussis* and *B. parapertussis*, and by other adhesin proteins from other organisms, a set of sequences deposited in the Uniprot database was aligned to compare epitope sequences.

This analysis showed that, in total, fourteen epitopes were unique to *B pertussis* (Ep1, Ep2, Ep3, Ep17, E18, Ep23, Ep25-Ep32). The S1 presented three (Ep1-Ep3), the S2 two (Ep17 and Ep18), the S3 two (Ep25 and Ep26), and all the epitopes from S4 and all the S5 (Ep31-Ep32) (Table S1). The high

 doi:10.20944/preprints202602.1259.v1



conservation of epitope structure suggests that strong cross-immunity occurs upon immunization with *B. pertussis* and B. *parapertussis* toxin preparations.

### *3.7. Search for Similar Epitope Sequences in the Data Bank*

A literature search showed that some Ptx epitopes had been previously identified using monoclonal antibodies or rabbit immunized sera (Table 1). Our epitope mapping revealed twelve (S1-5, S2-2, S3-2 S4-1 and S5-2) new murine and sixteen (S1-6, S2-3, S3-5 and S5-4) new human epitopes.

The epitopes recognized by chVs [S1 (Ep1,6,8); S3 (Ep22-Ep24); S4 (Ep27); S5 (Ep31, Ep32)] were unique based on sequence homology in the database. Four of these distinct epitopes were identified in the S2 subunit for each species [mice Ep11,14,16,17 and children Ep12,13,15,18], and only one in the S4 subunit (murine Ep 28).

### *3.8. Correlation of Ptx within Bordetella sp*

Since adhesin structures are highly conserved, proteins in this class are expected to exhibit structural similarity. As shown in Figure S2, the PtxS1-S5 proteins each harbor a set of linear epitopes that are also present in other Bordetella adhesin proteins.

Our analysis identified 11 *B. pertussis* epitopes that share sequences with the *B. parapertussis* toxin. However, these epitopes were recognized differently by vaccined mouse and child sera. The epitopes recognized by chVs that share sequences with *B. parapertussis* are Ep4-7, Ep12, Ep13, Ep15, Ep16, Ep20-24, and those recognized by miVs are Ep4, Ep5, Ep7, Ep9-11, Ep14, Ep16, Ep19-21 (Table 1).

However, a set of nine epitopes (Ep 1, Ep3, Ep18, Ep25, Ep26, Ep28, and Ep30-32) from *B. pertussis* recognized by chVs does not share sequence with the toxin of *B. parapertussis.*

## 4. Discussion

In this study, we performed a comprehensive linear B-cell epitope mapping of the five subunits of pertussis toxin (PtxS1–S5) using sera from whole-cell pertussis–vaccinated mice and children. By combining SPOT-synthesis peptide arrays, quantitative chemiluminescent detection, and structural modeling, we identified 32 IgG-reactive linear epitopes and demonstrated marked qualitative and quantitative differences between murine and human antibody repertoires. These findings provide mechanistic insight into interspecies differences in pertussis immunity and have direct implications for vaccine design, diagnostics, and translational modeling.

Pertussis toxin comprises five subunits (S1–S5) organized into two functional components: the toxic A subunit (S1) and the B subunit, which mediates receptor binding and consists of S2, S3, S5, and two S4 molecules. The assembly is stabilized by S5, which connects the S2–S4 and S3–S4 dimers. Consistent with previous reports, murine immunization with whole-cell pertussis vaccines elicited a focused antibody response preferentially targeting conserved and surface-exposed linear regions of the B-oligomer subunits S2, S3, and S4 [32,38–40]. The Ep3 sequence recognized by murine antibodies does not appear to fully block PtxS1 enzymatic activity, as only two residues (63 and 64) in site 1 of the active center were identified (Table 1). However, it is possible that the murine antibody binding to a site adjacent to the active center blocks substrate access or causes steric hindrance. This is consistent with previous findings that several monoclonal antibodies may block ADP ribosylation *in vitro* but are not neutralizing *in vivo* [41].

In fact, the predominance of murine epitopes in these subunits also aligns with earlier studies showing that mice tend to recognize linear peptide determinants on the toxin surface that are associated with receptor binding rather than enzymatic activity [42,43]. This pattern likely reflects species-specific constraints on the B-cell repertoire and antigen-processing pathways, as well as the Th1(IFN-¥)/Th17 (IL-17)-biased immune milieu induced by whole-cell vaccination in mice [44,45].

 doi:10.20944/preprints202602.1259.v1



In contrast, sera from vaccinated children recognized a broader array of linear epitopes across all five Ptx subunits, with a clear enrichment in the S1 enzymatic domain (essential for toxicity) and in regions proximal to known receptor-binding interfaces (adhesion) in S2 and S3 [31,33,35]. This broader recognition profile is consistent with prior observations that human immune responses to Ptx frequently include antibodies directed against enzymatically active and functionally neutralizing regions of the toxin [46–48]. Notably, thirteen epitopes were uniquely identified by children's sera, many of which have not been previously reported (Table 1 and Table S1), underscoring the greater diversity and complexity of the human antibody response to Ptx.

The limited overlap between murine and human epitope repertoires further highlights the challenges of extrapolating antibody specificity data from animal models to human immunity. Only a subset of epitopes, particularly within PtxS1, PtxS3, and PtxS5, were commonly recognized by both species. This partial convergence suggests that while mice remain a valuable model for identifying conserved and immunogenic linear determinants, they may underrepresent epitopes associated with toxin neutralization and long-term protection in humans [48,49]. These findings reinforce prior concerns about the translational limitations of murine pertussis models when used in isolation [47,48].

Structural mapping of the identified epitopes revealed that most localized to loop and coil regions exposed on the surface of the mature Ptx holotoxin, consistent with crystallographic data and hydropathy predictions [49,50]. The surface accessibility of these epitopes supports their biological relevance and explains their immunodominance following vaccination. Importantly, several human-specific epitopes mapped to regions involved in enzymatic activity or receptor engagement [51–53], providing a plausible mechanistic basis for the higher neutralizing capacity often observed in human anti-Ptx antibodies.

The structural patterns observed in this study are highly consistent with the mechanistic framework recently described using cryo-EM, which identified that a neutralizing antibody binds to Ptx. The structural analysis of the two humanized monoclonal antibodies studied, hu11E6 and hu1B7, that target distinct functional epitopes on genetically detoxified PT (PTg), with hu11E6 binding a conserved epitope on the paralogous S2 and S3 subunits to block toxin adhesion to sialylated receptors, thereby preventing cell binding and mitogenic activity, whereas hu1B7 engages a epitope spanning the S1 and S5 subunits and neutralizes PT through interference with its intracellular activity rather than through S5 contact itself [54]. Our quantitative and structural analyses corroborate this model by revealing a dominant antibody-binding bias toward the S3 subunit, followed by S2 and S4, consistent with the preferential targeting of structurally exposed and immunodominant regions. The recurrence of antibody engagement at specific epitope hotspots (notably Ep23 and Ep24) further supports the concept of conserved antigenic surfaces that accommodate diverse neutralizing antibodies.

Importantly, the identification of Ep4-binding hu1B7 on the S1 subunit extends the observations of previous work [54] by providing additional structural evidence for direct catalytic-domain targeting as a neutralization strategy.

These structural findings have direct implications for the design of acellular pertussis vaccines. As highlighted in Figure 7, epitopes proximal to/or overlapping the catalytic center, particularly Ep3, Ep4, and Ep5, represent high-value targets for structure-guided immunogen development. Incorporating or enhancing such epitopes in vaccine antigens may preferentially elicit antibodies with true neutralizing capacity rather than antibodies that bind without functional inhibition. This approach aligns with emerging strategies to improve the effectiveness of acellular pertussis vaccines by focusing immune responses on mechanistically relevant regions of the toxin.

Overall, integrating structural modeling with epitope-level immunological data supports a mechanism-driven framework for vaccine optimization, in which antibody responses are directed toward active-site–associated epitopes that directly impair toxin function.

In addition, the analysis of epitope conservation across Bordetella species demonstrated that while many epitopes are shared between *B. pertussis* and *B. parapertussis*, a distinct subset, particularly

 doi:10.20944/preprints202602.1259.v1



within PtxS1 and PtxS5, was unique to *B. pertussis*. These species-specific epitopes, predominantly recognized by children's sera, may contribute to differential cross-protection and could be exploited to improve diagnostic specificity or to develop next-generation vaccine formulations [54]. Conversely, the high conservation of several epitopes supports the concept of partial cross-immunity between *Bordetella* species following whole-cell vaccination, as previously suggested [55–57].

Our findings also expand the current epitope landscape of Ptx. Comparison with previously described monoclonal antibody and rabbit antisera studies identified 12 novel murine and 16 novel human linear epitopes. This expanded repertoire provides a valuable resource for rational antigen selection, particularly for epitope-based vaccines and serological assays that distinguish vaccine-induced from infection-induced immunity.

## 5. Conclusions

This study provides a comprehensive linear B-cell epitope map of pertussis toxin across all five subunits, revealing pronounced qualitative differences in antibody responses between murine and human vaccination. While mice predominantly targeted conserved, surface-exposed epitopes within the B-oligomer subunits S2, S3, and S4, vaccinated children exhibited broader epitope recognition, with marked enrichment in the S1 enzymatic domain and functionally relevant regions of the toxin.

These findings provide a mechanistic basis for differences in toxin neutralization and highlight limitations in extrapolating murine epitope data to human immunity.

Together, our results support a structure-guided approach to pertussis vaccine design that prioritizes active-site–associated epitopes with demonstrated neutralizing capacity and expands the epitope framework available for improved diagnostics and translational modeling.

**Supplementary Materials:** The following supporting information can be downloaded at: www.mdpi.com/xxx/s1, Figure S1. List of overlapping 15-mer peptides derived from all subunits of *Bordetella pertussis* toxin (PTx) and analyzed by SPOT-synthesis. Peptides were designed to comprehensively cover the full-length sequences of each toxin subunit, with sequential overlap to ensure continuous epitope mapping. Each peptide corresponds to a defined position within its respective subunit and was synthesized on cellulose support for antibody-binding analysis. This approach enabled the systematic identification of linear B-cell epitopes across the entire pertussis toxin complex.; Table S1. UniProt-reviewed bacterial toxins and homologous adhesins were analyzed for potential epitope cross-reactivity. The dataset comprises the following UniProt entries: P01555, P01556, P43530, P32890, P08191, P13430, P43261, Q5HD51, Q53653, and Q53654. The IEDB epitope similarity analysis shows the percentage of protein sequences that match known epitopes at ≤50% identity.

**Author Contributions:** Conceptualization, F.R.S and S.G.S.; methodology, P.N.P., G.C.L. and F.R.S.; writing original draft preparation, S.G.D-S.; writing review and editing, S.G.D-S.; visualization, F.R.S..; project administration, S.G.D-S.; funding acquisition, S.G.D-S. All authors have read and agreed to the published version of the manuscript.

**Funding:** This research was funded by Carlos Chagas Filho Foundation of Research Support of the State of Rio de Janeiro (FAPERJ #010.101.029/2018).

**Institutional Review Board Statement:** The study was approved by UNIGRANRIO (CAAE: 24856619.0.0000.5283) on 25 November 2019 and (CEP 052/2021) on 8 March 2022, the study center ethics committee, and was conducted in accordance with Good Clinical Practice and all applicable regulatory requirements, including the Declaration of Helsinki.

**Informed Consent Statement:** Not applicable.

**Data Availability Statement:** The data presented in this study are available on request from the corresponding author.

 doi:10.20944/preprints202602.1259.v1



**Acknowledgments:** We thank the National Institute of Quality Control (INCQs) from FIOCRUZ for their support with the vaccine and animal immunization. P.D-S.G. is a DrSci. CAPES fellow from the Post-Graduation Program on Science and Biotechnology, Federal Fluminense University.

**Conflicts of Interest:** The authors declare no conflict of interest.

## References

1. Melvin, J.; Scheller, E.; Miller, J.; Cotter, P.A. *Bordetella pertussis* pathogenesis: current and future challenges. *Nat Rev Microbiol* **2014**, *12*, 274–288. https://doi.org/10.1038/nrmicro3235.
2. Carbonetti, N.H. Contribution of pertussis toxin to the pathogenesis of pertussis disease. *Pathog Dis* **2015**, *73*, ftv073. https://doi.org/10.1093/femspd/ftv073.
3. Locht, C.; Antoine, R. The history of pertussis toxin. *Toxins* (Basel). **2021,** *13*, 623. https://doi.org/10.3390/toxins 13090623.
4. Wanlapakorn, N.; Maertens, K.; Vongpunsawad, S.; Puenpa, J.; Tran, T.M.P.; Hens, N.; Van Damme, P.; Thiriard, A.; Raze, D.; Locht, C.; et al., Quantity and quality of antibodies after acellular versus whole-cell pertussis vaccines in infants born to mothers who received tetanus, diphtheria, and acellular pertussis vaccine during pregnancy: A Randomized trial. *Clin Infect Dis* **2020**, *71*, 72-80. https://doi.org/10.1093/cid/ciz778.
5. Knuutila, A.; Dalby, T.; Barkoff~, A.M.; Jørgensen, C.S.; Fuursted, K.; Mertsola, J.; Markey, K.; He, Q. Differences in epitope-specific antibodies to pertussis toxin after infection and acellular vaccinations. *Clin Transl Immunology* **2020**, *9*, e1161. https://doi.org/10.1002/cti2.1161.
6. Duda-Madej, A.; Łabaz, J.; Topola, E.; Bazan, H.; Viscardi, S. Pertussis-a re-emerging threat despite immunization: an analysis of vaccine effectiveness and antibiotic resistance. *Int J Mol Sci* **2025,** *26*, 9607. https://doi.org/10.3390/ijms26199607.
7. Valeri, V.; Sochon, A.; Cousu, C.; Chappert, P.; Lecoeuche, D.; Blanc, P.; Weill, J.C.; Reynaud, C.A. The whole-cell pertussis vaccine imposes a broad effector B cell response in mouse heterologous prime-boost settings. *JCI Insight* **2022,** *7*, e157034. https://doi.org/10.1172/jci.insight.157034.4.
8. Lavigne, M.V.; Castro, M.; Mateo, N.; Deluchi, S.; Atzori, C.; Piudo, L.; Calcagno, M.; Brero, M.L.; Manghi, M. Whole-cell *Bordetella pertussis* vaccine component modulates the mouse immune response to an unrelated soluble antigen. *Microbes Infect* **2002**, *4*, 815-820. https://doi.org/10.1016/s1286-4579(02)01601-5.
9. Gzyl, A.; Augustynowicz, E.; Zawadka, M.; Rabczenko, D.; Slusarczyk, J. Analysis of chosen parameters of immune response in mice immunized with whole-cell or acellular pertussis vaccines and challenged with *B. pertussis* strains harboring different ptxS1/prn allele gene combinations. *Med Dosw Mikrobiol* **2007,** *59*, 137-147.
10. Knuutila, A.; Dalby, T.; Barkoff, A.M.; Jørgensen, C.S.; Fuursted, K.; Mertsola, J.; Markey, K.; He, Q. Differences in epitope-specific antibodies to pertussis toxin after infection and acellular vaccinations. *Clin Transl Immunology* **2020**, *9*, e1161. https://doi.org/10.1002/cti2.1161.
11. Sato, H.; Sato, Y.; Ito, A.; Ohishi, I. Protection and antibody responses after *Bordetella pertussis* infection in mice show that PT-specific IgA is produced in lungs following infection. *Infect Immun*. **2001**, 69, 1254–1259.
12. Boehm, D.T.; Wolf, M.A.; Hall, J.M.; Wong, T.Y.; Sen-Kilic, E.; Basinger, H.D.; Dziadowicz, S.A.; Gutierrez, M.P.; Blackwood, C.B.; Bradford, S.D.; et al., Intranasal acellular pertussis vaccine provides mucosal immunity and protects mice from *Bordetella pertussis*. *NPJ Vaccines* **2019,** *4*, 40. https://doi.org/10.1038/s41541-019-0136-2.
13. Solans, L.; Debrie, AS.; Borkner, L.; Borkner, L.; Aguiló, N.; Thiriard, A.; Coutte, L.; Uranga, S.; Trottein, F.; Martín, C.; et al., IL-17-dependent SIgA-mediated protection against nasal *Bordetella pertussis* infection by live attenuated BPZE1 vaccine. *Mucosal Immunol* **2019,** *11*, 1753–1762. doi: 10.1038/s41385-018-0073-9.
14. Dubois, V.; Locht, C. Mucosal immunization against pertussis: lessons from the past and perspectives. *Front Immunol* **2021,** *12*, 701285. https://doi.org/10.3389/fimmu.2021.701285.
15. Guo, M.; Li, H.; Meng, Q.; Wang, Y.; Chen, S.; Jia, Y.; Li, Q.; Sun, M.; Yao, K. Adult pertussis in the acellular-cell vaccine era: Comparative analysis of pertussis toxin antibodies in hospitalized patients with prolonged cough. *Hum Vaccin Immunother* **2025**, *21*, 2521915. https://doi.org/10.1080/21645515.2025.2521915.

 doi:10.20944/preprints202602.1259.v1




16. Wu, Y.; Gan, C. Impact of pertussis vaccination on PT-IgG levels and clinical characteristics in 3-12-month-old infants with acute pertussis. *Eur J Pediatr* **2025**,*184*, 501. https://doi.org/10.1007/s00431-025-06328-w.
17. Schmidt, W.; Schmidt, M.A. Mapping of linear B-cell epitopes of the S2 subunit of pertussis toxin. *Infect Immun* **1989**, *57*, 438-445. https://doi.org/10.1128/iai.57.2.438-445.
18. Goldsmith, J.A.; Nguyen, A.W.; Wilen, R.E.; Wijagkanalan, W.; McLellan, J.S.; Maynard, J.A. Structural basis for neutralizing antibody binding to pertussis toxin. *Proc Natl Acad Sci* U S A. **2025**, *122*, e2419457122. https://doi.org/10.1073/pnas.2419457122.
19. Burns, D.L.; Fiddner, S.; Cheung, A.M.; Verma, A. Analysis of subassemblies of pertussis toxin subunits in vivo and their interaction with the ptl transport apparatus. *Infect Immun* **2004**, *72*, 5365-5372. https://doi.org/10.1128/IAI.72.9.5365-5372.2004.
20. Felici, F.; Luzzago, A.; Folgori, A.; Cortese, R. Mimicking of discontinuous epitopes by phage-displayed peptides, II. Selection of clones recognized by a protective monoclonal antibody against the *Bordetella pertussis* toxin from phage peptide libraries. *Gene* **1993,** *128*. 21-27. https://doi.org/10.1016/0378-1119(93)90148-v.
21. Giuliano, M.; Mastrantonio, P.; Giammanco, A.; Piscitelli, A.; Salmaso, S.; Wassilak, S.G. Antibody responses and persistence in the two years after immunization with two acellular vaccines and one whole-cell vaccine against pertussis. *J Pediatr* **1998,** *132*, 983-988. https://doi.org/10.1016/s0022-3476(98)70395-6.
22. Sutherland, J.N.; Maynard, J.A. Characterization of a key neutralizing epitope on pertussis toxin recognized by monoclonal antibody 1B7. *Biochemistry.* **2009**, *48*, 11982-93. https://doi.org/10.1021/bi901532z.
23. Abu-Raya, B.; Esser, M.J.; Nakabembe, E.; Reiné, J.; Amaral, K.; Diks, A.M.; Imede, E.; Way, S.S.; Harandi, A.M.; Gorringe, A.; et al., Antibody and B-cell immune responses against *Bordetella pertussis* following infection and immunization. *J Mol Biol* **2023**, *435*, 168344. https://doi.org/10.1016/j.jmb.2023.168344.
24. Knuutila, A.; Dalby, T.; Ahvenainen, N.; Barkoff, A.M.; Jørgensen, C.S.; Fuursted, K.; Mertsola, J.; He, Q. Antibody avidity to pertussis toxin after acellular pertussis vaccination and infection. *Emerg Microbes Infect* **2023,** *12*, e2174782. https://doi.org/10.1080/22221751.2023.2174782.
25. Brandon, D.; Kimmel, M.; Kuriyakose, S.O.; Kostanyan, L.; Mesaros, N. Antibody persistence and safety and immunogenicity of a second booster dose nine years after a first booster vaccination with a reduced antigen diphtheria-tetanus-acellular pertussis vaccine (Tdap) in adults. *Vaccine* **2018**, *36*, 6325-6333. https://doi.org/10.1016/j.vaccine.2018.08.051. Erratum in: *Vaccine* **2020**, *38*, 2746-2747. https://doi.org/10.1016/j.vaccine.2020.01.082.
26. Mills, K.H.G.; Ryan, M.; Ryan, E.; Mahon, B.P. A murine model in which protection correlates with pertussis vaccine efficacy in children reveals complementary roles for humoral and cell-mediated immunity. *Infect Immun* **1998**, *66*, 594–602. https://doi.org/10.1128/IAI.66.2.594-602.1998.
27. Barkoff, A.M.; Knuutila, A.; Mertsola, J.; He, Q. Evaluation of anti-PT antibody response after pertussis vaccination and infection: The importance of both quantity and quality. *Toxins* (Basel) **2021**, *13*, 508. https://doi.org/10.3390/toxins13080508.
28. da Silva, F.R.; Napoleão-Pego, P.; De-Simone, S.G. Identification of linear B epitopes of pertactin of *Bordetella pertussis* induced by immunization with whole and acellular vaccine. *Vaccine* **2014**, *32*, 6251-6258. https://doi.org/10.1016/j.vaccine.2014.09.019.
29. De-Simone, S.G.; Gomes, L.R.; Napoleão-Pêgo, P.; Lechuga, G.C.; de Pina, J.S.; da Silva, F.R. Epitope mapping of the diphtheria toxin and development of an ELISA-specific diagnostic assay. *Vaccines* (Basel). **2021**, *9*, 313. https://doi.org/10.3390/vaccines9040313.
30. De-Simone, S.G.; Napoleão-Pêgo, P.; Lechuga, G.C.; Carvalho, J.P.R.S.; Gomes, L.R.; Cardoso, S.V.; Morel, C.M.; Provance-Jr, D.W.; Silva, F.R.S. High-throughput IgG epitope mapping of tetanus neurotoxin: implications for immunotherapy and vaccine design, *Toxins* (Basel) **2023,** 15, 239. https://doi.org/10.3390/toxins 15040239.
31. Jumper, J.; Evansm, R.; Pritzel, A.; Green, T.; Figurnov, M.; Ronneberger, O.; Tunyasuvunakool, K.; Bates, R.; Žídek, A.; Potapenko, A.; et al. Highly accurate protein structure prediction with AlphaFold. *Nature* **2021**, *596*, 583–589. https://doi.org/10.1038/s41586-021-03819-2.

 doi:10.20944/preprints202602.1259.v1




32. Chong, P.; Chan, C.; Lewis, C.; Liu, W.; DeWolf, M.; Klein, M. Identification of T- and B-cell epitopes of the S2 and S3 subunits of pertussis toxin using synthetic peptides. *Infect. Immun.* **1991**, *59*, 396–402. https://doi.org/10.1128/iai.60.11.4640-4647.1992
33. Raupach, B.; Schmidt, M.A. Elucidation of linear epitopes of pertussis toxin using overlapping synthetic decapeptides: identification of an infant's B-cell determinant in the S1 subunit indicative of acute infections. *Microb Pathogen* **1994,** *17*, 213-226. https://doi.org/10.1006/mpat.1994.1067.
34. Askelöf, P.; Rodmalm, K.; Abens, J.; Undén, A.; Bartfai, T. Use of synthetic peptides to map antigenic sites of *Bordetella pertussis* toxin subunit S1. *J Infect Dis* **1988,** *157*, 738-742**. https://doi.org/**10.1093/infdis/157.4.738.
35. Chong P, Zobrist G, Sia C, Loosmore S, Klein M. Identification of T- and B-cell epitopes of the S2 and S3 subunits of pertussis toxin by use of synthetic peptides. *Infect Immun* **1992**, *60*, 4640-4647. https://doi.org/10.1128/iai. 60.11.4640-4647.1992.
36. Hazes, B.; Boodhoo, A.; Cockle, S.A.; Read, R.J. Crystal structure of the pertussis toxin-ATP complex: a molecular sensor. *J Mol Biol* **1996**, *258*, 661-671. https://doi.org/10.1006/jmbi.1996.0277**.**
37. Sakari M, Tran MT, Rossjohn J, Pulliainen AT, Beddoe T, Littler DR. Crystal structures of pertussis toxin with $NAD^+$ and analogs provide structural insights into the mechanism of its cytosolic ADP-ribosylation activity. *J Biol Chem* **2022,** *298*, 101892. https://doi.org/10.1016/j.jbc.2022.101892.
38. Schmidt, W.; Schmidt, M.A. Mapping of linear B-cell epitopes of the S2 subunit of pertussis toxin. Infect. Immun. **1989**, 57, 438–445.
39. Schmidt, M.A.; Raupach, B.; Szulczynski, M.; Marzillier, J. Identification of linear B-cell determinants of pertussis toxin associated with the receptor recognition site of the S3 subunit. *Infect. Immun.* **1991**, *59*, 1402–1408.
40. Ibsen, P.H.; Holm, A.; Petersen, J.W.; Olsen, C.E.; Heron, I. Identification of B-cell epitopes on the S4 subunit of pertussis toxin. *Infect Immun.* **1993,** *61*, 2408-2418. https://doi.org/10.1128/iai.61.6.2408-2418.1993.
41. Arciniega, J.L.; Burns, D.L.; Garcia-Ortigoza, E.; Manclark, C.R. Immune response to the B oligomer of pertussis toxin. *Infect. Immun.* **1987**, *55*, 1132–1136. https://doi.org/10.1128/iai.55.5.1132-1136.1987.
42. Valeri, V.; Sochon, A.; Kuper, C.F.; et al. The whole-cell pertussis vaccine imposes a broad effector B cell response in mouse heterologous prime–boost settings. *JCI Insight* **2022**, *7*, e157034. https://doi.org/10.1172/ jci.insight.157034.
43. Acquaye-Seedah, E.; Huang, Y.; Sutherland, J.N.; DiVenere, A.M.; Maynard, J.A. Humanised monoclonal antibodies neutralise pertussis toxin by receptor blockade and reduced retrograde trafficking. *Cell Microbiol* **2018,** *20*, e12948. https://doi.org/10.1111/cmi.12948.
44. Mills, K.H.; Barnard, A.; Watkins, J.; Redhead, K. Cell-mediated immunity to *Bordetella pertussis*: role of Th1 cells in bacterial clearance in a murine respiratory infection model. *Infect Immun* **1993**, *61*, 399–410. https://doi.org/10.1128/iai.61.2.399-410.1993.
45. Barnard, A.; Mahon, B.P.; Watkins, J.; Redhead, K.; Mills, K.H. Th1/Th2 cell dichotomy in acquired immunity to *Bordetella pertussis:* variables in the in vivo priming and in vitro cytokine detection techniques affect the classification of T-cell subsets as Th1, Th2, or Th0. *Immunology* **1996**, *87*, 372-380. https://doi.org/10.1046/ j.1365-2567.1996.497560.x.
46. Kaslow, H.R.; Platler, B.W.; Blumberg, D.A.; Cherry, J.D. Detection of antibodies inhibiting the ADP-ribosyltransferase activity of pertussis toxin in human serum. *J Clin Microbiol* **1992,** *30*, 1380-1387. https://doi.org/10.1128/jcm.30.6.1380-1387.1992.
47. Saso, A.; Kampmann, B.; Roetynck, S. Vaccine-induced cellular immunity against *Bordetella pertussis:* harnessing lessons from animal and human studies to improve design and testing of novel pertussis vaccines. *Vaccines* (Basel) **2021**, *9*, 877. https://doi.org/10.3390/ vaccines9080877.
48. Wang, X.; Gray, M.C.; Hewlett, E.L.; Maynard, J.A. The Bordetella adenylate cyclase repeat-in-toxin (RTX) domain is immunodominant and elicits neutralizing antibodies. *J Biol Chem* **2015**, *290*,3576-3591. https://doi.org/10.1074/jbc.M114.585281. Erratum in: *J Biol Chem* **2015,** *290*, 23025. https://doi.org/10.1074/jbc.A114.585281.
49. Soumana, I.H.; Linz, B.; Dewan, K.K.; Sarr, D.; Gestal, M.C.; Howard, L.K.; Caulfield, A.D.; Rada, B.; Harvill, E.T. Modeling immune evasion and vaccine limitations by targeted nasopharyngeal *Bordetella pertussis* inoculation in mice. *Emerg Infect Dis* **2021**, *27*, 2107-2116. https://doi.org/10.3201/eid2708.203566**.**

 doi:10.20944/preprints202602.1259.v1




50. Nguyen, A.W.; Wagner, A.; Bui, P.; Sato, Y.; Maynard, J.A. Synergistic neutralization of pertussis toxin by humanized antibodies targeting distinct functional sites. *mAbs* **2016**, *8*, 884–896. https://doi.org/10.1080/19420862.201 6.1199308.
51. Sato, Y.; Wagner, A.; Bui, P.; et al. Humanised monoclonal antibodies neutralise pertussis toxin by receptor blockade and altered intracellular trafficking. Sci. Rep. 2019, 9, 12301. https://doi.org/10.1038/s41598-019-48607-4
52. van der Lee, A.H.; McGinley, M.P.; Wilen, R.E.; Goldsmith, J.A.; Maynard, J.A. Characterization of individual human antibodies that bind pertussis toxin stimulated by acellular immunization. *PLoS ONE* **2018**, *13*, e0208310. https://doi.org/10.1128/IAI.00004-18.
53. Goldsmith, J.A.; Nguyen, A.W.; Wilen, R.E.; Wijagkanalan, W.; McLellan, J.S.; Maynard, J.A. Structural basis for neutralizing antibody binding to pertussis toxin. *Proc. Natl. Acad. Sci. USA* **2024**, *121*, e2419457121. https://doi.org/10.1073/pnas.2419457122.
54. Zhang, X.; Weyrich, L.S.; Lavine, J.S.; Karanikas, A.T.; Harvill, E.T. Lack of cross-protection against *Bordetella holmesii* after Pertussis vaccination. *Emerg Infect Dis* **2012**, *18*, 11-1544. https://doi.org/10.3201/eid1811.111544.
55. Moore, J.E.; Rendall, J.C.; Millar, B.C. Does *Bordetella pertussis* vaccine offer any cross-protection against *Bordetella bronchiseptica*? Implications for pet owners with cystic fibrosis. *J Clin Pharm Ther.* **2021,** *46*, 1194-1198. https://doi.org/10.1111/ jcpt.1335057
56. Natrajan, M.S.; Hall, J.M.; Weigand, M.R.; Peng, Y.; Williams, M.M.; Momin, M.; Damron, F.H.; Dubey, P.; Tondella, M.L.; Pawloski, L.C. Genome-based prediction of cross-protective, HLA-DR-presented epitopes as putative vaccine antigens for multiple Bordetella species. *Microbiol Spectr* **2023,** *12*, e03527-23. https://doi.org/10.1128/spectrum.03527-23.